

Research Article

Thermal Effect on the Structural, Electrical, and Optical Properties of In-Line Sputtered Aluminum Doped Zinc Oxide Films Explored with Thermal Desorption Spectroscopy

Shang-Chou Chang, Tien-Chai Lin, and To-Sing Li

Department of Electrical Engineering, Kun Shan University, Tainan 71003, Taiwan

Correspondence should be addressed to Shang-Chou Chang; jchang@mail.ksu.edu.tw

Received 7 May 2014; Accepted 18 May 2014; Published 29 May 2014

Academic Editor: Teen-Hang Meen

Copyright © 2014 Shang-Chou Chang et al. This is an open access article distributed under the Creative Commons Attribution License, which permits unrestricted use, distribution, and reproduction in any medium, provided the original work is properly cited.

This work investigates the thermal effect on the structural, electrical, and optical properties of aluminum doped zinc oxide (AZO) films. The AZO films deposited at different temperatures were measured using a thermal desorption system to obtain their corresponding thermal desorption spectroscopy (TDS). In addition to obtaining information of thermal desorption, the measurement of TDS also has the effect of vacuum annealing on the AZO films. The results of measuring TDS imply part of the doped aluminum atoms do not stay at substituted zinc sites in AZO films. The (002) preferential direction of the AZO films in X-ray diffraction spectra shifts to a lower angle after measurement of TDS. The grain size grows and surface becomes denser for all AZO films after measurement of TDS. The carrier concentration, mobility, and average optical transmittance increase while the electrical resistivity decreases for AZO films after measurement of TDS. These results indicate that the AZO films deposited at 200°C are appropriate selections if the AZO films are applied in device fabrication of heat-produced process.

1. Introduction

Zinc oxide is an old semiconductor material that dates back to the beginning of the 20th century. It has been applied in different areas like piezoelectric transducers, optical waveguides, acoustooptic media, gas sensors, varistors, and transparent conductive (TC) electrode [1]. The recent popular and hot application for zinc oxide is TC electrode. Indium tin oxide (ITO) is regularly used in TC electrode of light emitting diodes, flat panels, or solar cells industry [2]. Since indium is rare and toxic, there is a tendency to replace ITO with aluminum doped zinc oxide (AZO) for cost and safety concerns. These years, the AZO can compete with ITO due to compatible electrical and optical properties [3, 4]. In-line sputtering method can be used to produce large-area and high-throughput thin films. This work focuses on surveying in-line sputtered instead of batch-type produced AZO films. Anisotropic stress in thin films produced during in-line sputtering process has been reported [5]. The properties of AZO films produced by in-line sputtering may be different

when being compared with those produced by batch-type sputtering.

Heat generation may occur after TC electrode is produced in solar cells fabrication, such as plasma enhanced chemical vapor deposition in growing amorphous silicon films as absorption layer materials. The substrate temperature in the above process is usually around 300°C [6]. The structural, electrical, and optical properties of AZO films may change after the heat generation process. Haug et al. have reported AZO films' property alternation after thermal treatment [7]. Variation in electrical and optical properties of AZO films has to be considered if AZO films are used in heat production process.

Thermal desorption spectroscopy was firstly used in studying metal or gas desorption behavior [8]. More applications for TDS such as thermal stability [9], catalyst reaction [9], and hydrogen storage [10, 11] were developed recently. Our group has applied TDS to investigate the thermal effect on fluorine doped zinc oxide (ZnO:F) films before [12]. The results indicate ZnO:F films desorb corresponding to low

bound strength under heat treatment of 100°C. Fluorine is easily desorbed from ZnO:F films. Apparently, negative effects influence the electrical and optical properties of ZnO:F films during heating process. The electrical resistivity increases whereas the average optical transmittance in visible wavelength decreases for ZnO:F films after TDS measurement. The measurement of TDS is a heating process for ZnO:F films. This finding further motivates us to study the thermal effect on commonly used zinc oxide films: AZO films. This work applied TDS to study the thermal effect on the structural, electrical, and optical properties of AZO films deposited at different substrate temperatures. We checked whether there was any species desorbed from AZO films during measuring TDS and then calculated and compared the thermal desorption amount of AZO films. Structural, electrical, and optical properties of AZO films before and after TDS measurements were also explored.

2. Experimental Procedure

The substrate that AZO films were to be deposited on was the borosilicate glass. The $2.54 \times 2.54 \text{ cm}^2$ borosilicate glass was ultrasonically cleaned with purified water and acetone in sequence three times. After that, the glass was further cleaned with purified water and dried with dry nitrogen. One in-line DC magnetron sputtering tool was applied to deposit AZO films. The ceramic AZO target was with $\text{ZnO}/\text{Al}_2\text{O}_3 = 98:2 \text{ wt\%}$ in composition and $95 \times 20 \text{ cm}^2$ in size. The sputtering power density was $1.58 \text{ W}/\text{cm}^2$. The process chamber was pumped down to $5 \times 10^{-3} \text{ Pa}$ as base pressure. The process pressure was kept at $3 \times 10^{-1} \text{ Pa}$ with feeding pure argon. The substrate temperature during sputtering process was at room temperature (RT), 100°C, and 200°C, respectively. The film thickness of produced AZO films was 500 nm. The TDS of prepared AZO films were measured. The measurement system of TDS was pumped down to 10^{-5} Pa range or below. Then, the AZO films were linearly heated by a proportional-integral-derivative controller at a fixed 10°C per minute heating rate from RT to 500°C. The heating of the measurement system was closed after the AZO films reached 500°C. The temperature of the TDS measurement system was naturally cooled down in vacuum. Measuring TDS of the AZO films also plays the role of vacuum annealing on the AZO films. Ion currents corresponding to ion mass to charge ratio (m/e) 16, 27, 32, and 65 were measured with a quadrupole mass spectrometer (QMS). The m/e of 16, 27, 32, and 65 corresponds to the oxygen atom, aluminum atom, oxygen molecule, and zinc atom, respectively. The TDS of the AZO films was obtained by plotting ion currents of the above four elements versus the corresponding temperature.

The crystalline structure and surface morphology of AZO films before and after measuring TDS were probed with an X-ray diffractometer (XRD) and a scanning electron microscope (SEM), respectively. The carrier concentration, mobility, and electrical resistivity of AZO films before and after measuring TDS were obtained by a hall measurement with Van-Der Pauw method. The optical transmittance of

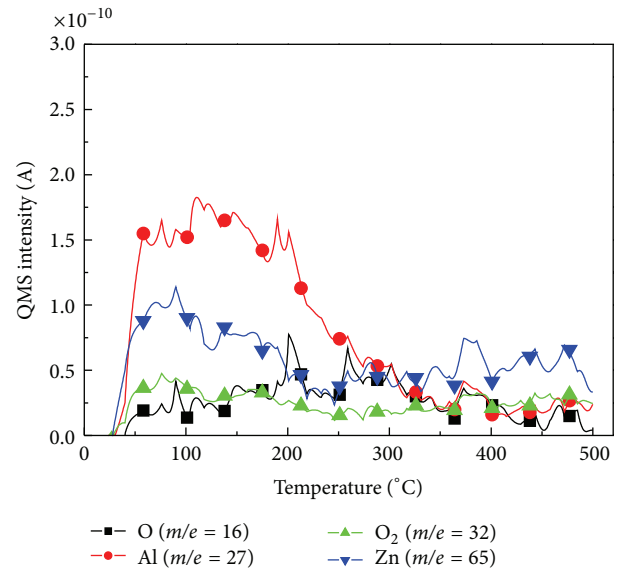


FIGURE 1: Thermal desorption spectroscopy of the AZO films deposited at 200°C.

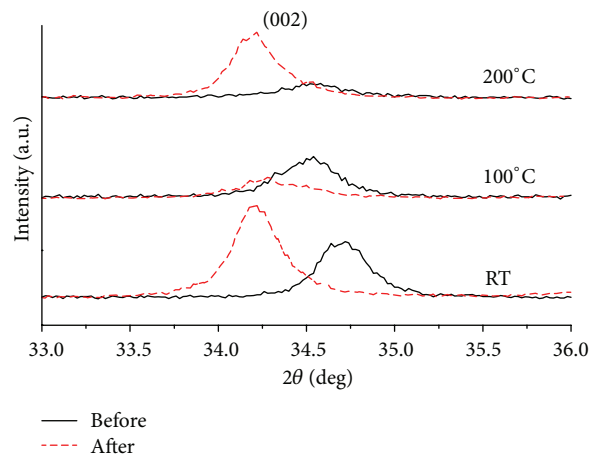


FIGURE 2: The X-ray diffraction spectra of the AZO films deposited at room temperature (RT), 100°C, and 200°C before and after measuring TDS.

AZO films before and after measuring TDS was probed by an ultraviolet-visible spectrophotometer. The percent variation of electrical resistivity and average optical transmittance in visible wavelength region for the AZO films before and after measuring TDS were calculated. The AZO films with low percent variation of electrical resistivity and optical transmittance imply they demonstrate stable electrical and optical properties when applied in heat production process.

3. Results and Discussion

3.1. Thermal Desorption. All AZO films deposited at different substrate temperatures exhibit similar curve shape but different intensity in TDS. The increasing ion current regarding

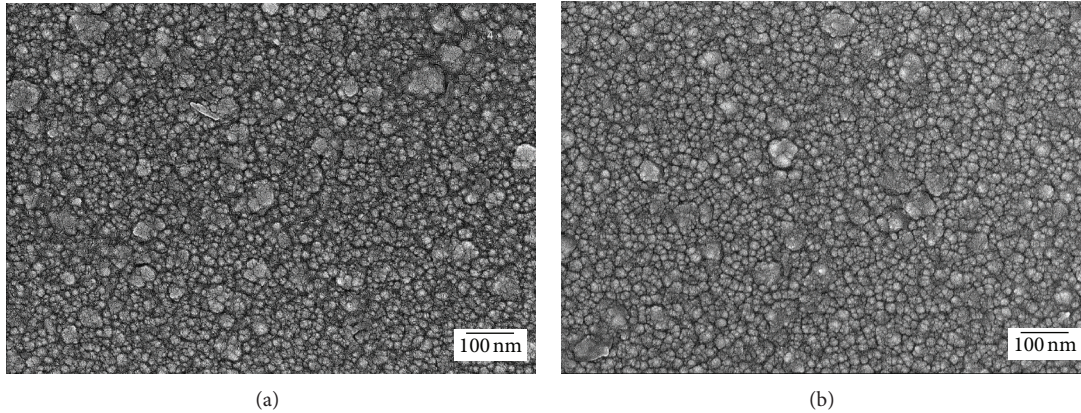


FIGURE 3: SEM micrographs of the AZO films deposited at room temperature (RT) (a) before and (b) after measuring TDS.

oxygen atom, aluminum atom, oxygen molecule, and zinc atom, respectively, can be apparently observed during TDS measurement. The TDS of the 200°C substrate produced AZO films was shown in Figure 1. The impurity metal element, aluminum atom, and the intrinsic metal element, zinc atom, both exhibit higher thermal desorption intensity than oxygen atom and oxygen molecule seen from Figure 1. The apparent increase in thermal desorption intensity of the four elements is between 60 and 200°C. High thermal desorption intensity of the aluminum atom indicates that aluminum is thermally unstable in AZO films. Haug et al. reported the thermal stability of extrinsic donors in zinc oxide like aluminum is better than that of intrinsic donors [7]. The thermal instability of aluminum found in this work may attribute that some aluminum atoms in AZO films do not exist in substituted zinc sites. They stay in other positions which make aluminum thermally unstable.

Thermal desorption amount of the elements in AZO films is proportional to integrating thermal desorption intensity with temperature derived from Polanyi-Wigner equation [8]. The ratio of desorption amount for the aluminum atom was calculated to be 39 : 26 : 22, corresponding to AZO films deposited at RT, 100°C, and 200°C substrate, respectively. This phenomenon may attribute that when AZO films deposited at high substrate temperature like 200°C, thermally unstable atoms or molecules have been thermally desorbed during sputtering. Therefore, the remaining materials on substrate after sputtering possess good adhesion. Good adhesion of the AZO films can reduce the possibility that the AZO constitutions diffuse to other layer(s) during device fabrication in heat-produced process if AZO films are applied as TC electrodes. The diffusion may deteriorate the device function.

3.2. Structural Property. All AZO films possess (002) preferential direction obtained from measuring X-ray diffraction. The X-ray diffraction spectra for the AZO films deposited at different substrate temperatures before and after measuring TDS are shown in Figure 2. The corresponding (002) peak location and full width at half maximum of X-ray diffraction spectra are listed in Table 1. After TDS being measured,

TABLE 1: The (002) peak location and full width at half maximum of X-ray diffraction spectra of the AZO films deposited at room temperature (RT), 100°C, and 200°C before and after measuring TDS.

| Substrate temperature | 2θ | | FWMH | |
|-----------------------|-----------|--------|--------|-------|
| | Before | After | Before | After |
| RT | 34.70° | 34.25° | 0.35° | 0.32° |
| 100°C | 34.54° | 34.20° | 0.40° | 0.44° |
| 200°C | 34.56° | 34.20° | 0.45° | 0.36° |

the (002) peak shifts to a lower angle for all AZO films. The measurement of TDS has the effect of vacuum annealing on the AZO films. It may cause the high proportion of metallic interstitial defects in the lattice of the AZO films [13]. This increases the lattice space which makes (002) peaks shift to a lower angle for the AZO films after TDS measurement. The full width at half maximum decreases for the AZO films deposited at RT and 200°C after measuring TDS. However, the full width at half maximum increases for the AZO films deposited at 100°C after measuring TDS. The measured results on the full width at half maximum of X-ray diffraction spectra for the AZO films may be related to grain growth and release of anisotropic stress. The measurement of TDS provides thermal energy to make the grains of the AZO films grow. However, it may also release the anisotropic stress for the AZO films produced during in-line sputtering [14]. Incomplete release of the anisotropic stress may explain the increment of the full width at half maximum for AZO films deposited at 100°C.

Figure 3 shows SEM micrographs of the AZO films deposited at RT before and after measuring TDS. The film surface of the AZO films after measuring TDS becomes relatively smooth as observed from Figure 3. Figure 4 shows the SEM observation of the AZO films deposited at 100°C, before and after measuring TDS. The grains are quite even for samples deposited at 100°C compared with those deposited at RT. Figure 5 shows the SEM observation of the AZO films deposited at 200°C, before and after measuring TDS.

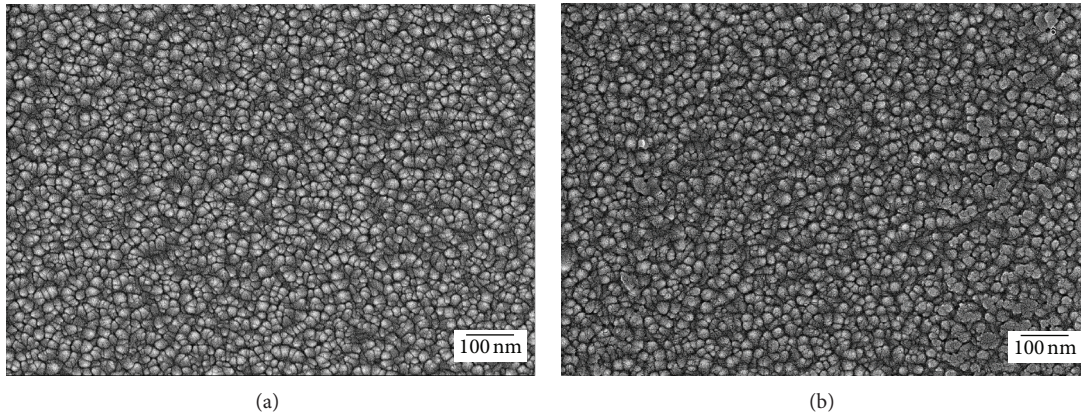


FIGURE 4: SEM micrographs of the AZO films deposited at 100°C (a) before and (b) after measuring TDS.

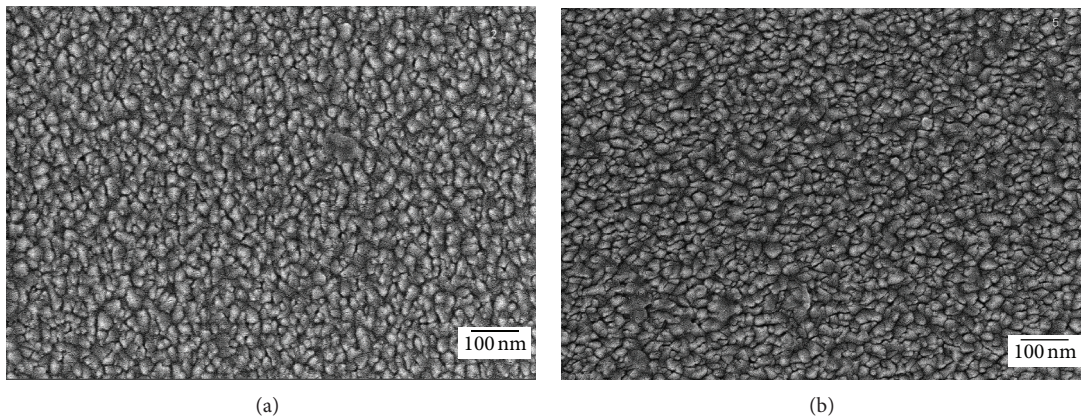


FIGURE 5: SEM micrographs of the AZO films deposited at 200°C (a) before and (b) after measuring TDS.

The surface morphology of the samples deposited at 200°C demonstrates a pyramidal shape. The grain size grows and surface becomes denser for all AZO films after measuring TDS as observed from Figures 3 to 5. The provision of thermal energy by TDS for grain growth of the AZO films is further evidenced by the results of the SEM micrographs.

3.3. Electrical Property. The electrical properties carrier concentration, mobility, electrical resistivity, and percent variation of electrical resistivity for the AZO films deposited at different temperatures before and after measuring TDS were shown in Table 2. The carrier concentration and mobility increase whereas the electrical resistivity decreases for the AZO films deposited at different temperatures after measuring TDS. The measurement of TDS has vacuum annealing effect on AZO films, and vacuum annealing effect causes more aluminum atoms to substitute zinc sites [15] or promotes desorption of oxygen from grain boundaries so as to increase the carrier concentration [16]. It makes AZO films increase oxygen defects, zinc interstitial atoms, and grain size [17]. Increase in oxygen defects and zinc interstitial atoms raises carrier concentration. The growth in grain size of

the AZO films results in less grain boundary scattering. The mobility of the AZO films is therefore increased.

The AZO films deposited at 200°C exhibit the lowest electrical resistivity before or after measuring TDS, as well as the lowest percent variation among the AZO films deposited at different temperatures seen from Table 2. These results indicate the AZO films deposited at 200°C are suitable selections applying in thermally treated process based on electrical properties. Poor electrical properties such as low carrier concentration and mobility and high percent variation of electrical resistivity for the AZO films deposited at 100°C before and after measuring TDS shown in Table 2 may be related with anisotropic stress in AZO films produced during in-line sputtering [14]. The stress resulted from skew incidence of sputtered ions or atoms' flux on substrate along the in-line moving direction when the substrate was entering or leaving the process chamber during sputtering. The direction perpendicular to the moving direction of substrate does not have the abovementioned stress. The anisotropic stress was trapped in AZO films when the films were deposited at RT. The anisotropic stress started to be released but incompletely when the films were deposited at 100°C. Poor crystalline structure of the AZO films deposited at 100°C was evidenced

TABLE 2: The electrical properties: carrier concentration, mobility, electrical resistivity, and percent variation of electrical resistivity of the AZO films deposited at room temperature (RT), 100°C, and 200°C before and after measuring TDS.

| Substrate temperature | Before | | | After | | | Electrical resistivity's percent variation (%) |
|-----------------------|---|---------------------------------------|---|---|---------------------------------------|---|--|
| | Carrier concentration (10^{20} cm^{-3}) | Mobility ($\text{cm}^2/\text{V-s}$) | Electrical resistivity ($10^{-4} \Omega\text{-cm}$) | Carrier concentration (10^{20} cm^{-3}) | Mobility ($\text{cm}^2/\text{V-s}$) | Electrical resistivity ($10^{-4} \Omega\text{-cm}$) | |
| RT | 3.7 | 6.4 | 27 | 4.1 | 8.0 | 19 | -30 |
| 100°C | 0.6 | 6.6 | 160 | 1.3 | 6.9 | 69 | -57 |
| 200°C | 6.0 | 6.4 | 16 | 6.9 | 7.5 | 12 | -25 |

TABLE 3: The average optical transmittance in visible wavelength region and the corresponding percent variation of the AZO films deposited at room temperature (RT), 100°C, and 200°C before and after measuring TDS.

| Substrate temperature | Average optical transmittance (%) | | Average optical transmittance's percent variation (%) |
|-----------------------|-----------------------------------|-------|---|
| | Before | After | |
| RT | 70 | 82 | 17 |
| 100°C | 71 | 75 | 5.6 |
| 200°C | 90 | 92 | 2.2 |

in results of the X-ray diffraction spectra in Figure 2 and Table 1. Poor crystalline structure destroys part of the carriers and lowers the mobility for the AZO films deposited at 100°C.

3.4. Optical Property. Figure 6 presents the optical transmittance spectra for the AZO films deposited at different temperatures before and after measuring TDS. Blue shift behavior of the optical transmittance spectra for the AZO films after measuring TDS was apparently observed in inset of Figure 6. The blue shift behavior can be ascribed to Burstein-Moss effect [18, 19]. The measurement of TDS which has the effect of vacuum annealing causes the increase of carrier concentration as shown in Table 2. The increment of carrier concentration widens the optical band gap of the AZO films. The average optical transmittance and the corresponding percent variation of the AZO films before and after measuring TDS deposited at RT, 100°C, and 200°C were shown in Table 3. The AZO films deposited at 200°C exhibit the highest average optical transmittance before or after measuring TDS and lowest percent variation among those deposited at different temperatures observed from Table 2. The measurement of TDS which has the effect of vacuum annealing reduces the materials defects of AZO films [20]; the average optical transmittance therefore increases.

4. Conclusion

Thermal effect on the structural, electrical, and optical properties of AZO films was studied by measuring TDS. The results of TDS imply part of the doped aluminum atoms do not stay at the substituted zinc sites in AZO films. The measurement of TDS has the effect of vacuum annealing on the AZO films. The measurement of TDS provides thermal energy to make the grains growth of the AZO films, and

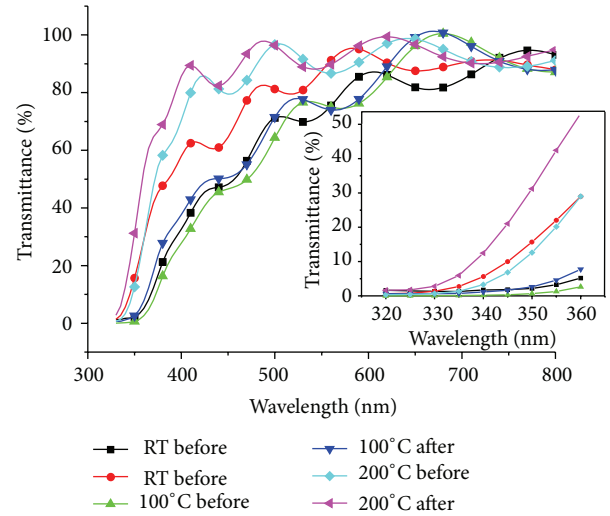


FIGURE 6: The optical transmittance spectra of the AZO films deposited at room temperature (RT), 100°C, and 200°C before and after measuring TDS.

such finding is evidenced by the results of the SEM micrographs. The carrier concentration, mobility, and average optical transmittance of the AZO films increase after measuring TDS. On the other hand, the electrical resistivity of the AZO films decreases after measuring TDS. The AZO films deposited at 200°C are appropriate selections if the AZO films are applied in device fabrication of heat-produced process. In short, the AZO films deposited at 200°C show low electrical resistivity, high average optical transmittance, low percent variation of electrical resistivity, and average optical transmittance among all tested AZO films.

Conflict of Interests

The authors declare that there is no conflict of interests regarding the publication of this paper.

Acknowledgments

The authors would like to thank the National Science Council of Taiwan for financial support (NSC-98-2221-E-168-005 and NSC 102-2221-E-168-037), Bay Zu Precision Corporation for providing in-line sputtering tool, and Shen-Hua Wu for carrying out part of measurements.

References

- [1] R. Triboulet and J. Perrière, "Epitaxial growth of ZnO films," *Progress in Crystal Growth and Characterization of Materials*, vol. 47, no. 2-3, pp. 65–138, 2003.
- [2] R. G. Gordon, "Criteria for choosing transparent conductors," *MRS Bulletin*, vol. 25, no. 8, pp. 52–57, 2000.
- [3] P. Nunes, E. Fortunato, P. Tonello, F. Braz Fernandes, P. Vilarinho, and R. Martins, "Effect of different dopant elements on the properties of ZnO thin films," *Vacuum*, vol. 64, no. 3-4, pp. 281–285, 2002.
- [4] R. J. Hong, X. Jiang, B. Szyszka, V. Sittinger, and A. Pflug, "Studies on ZnO:Al thin films deposited by in-line reactive mid-frequency magnetron sputtering," *Applied Surface Science*, vol. 207, no. 1–4, pp. 341–350, 2003.
- [5] S. Suzuki, "Internal stress and adhesion of thin films sputtered onto glass by an in-line sputtering system," *Thin Solid Films*, vol. 351, no. 1-2, pp. 194–197, 1999.
- [6] J. Cárabe and J. J. Gandia, "Thin-film-silicon solar cells," *Optoelectronics Review*, vol. 12, no. 1, pp. 1–6, 2004.
- [7] F.-J. Haug, Z. Geller, H. Zogg, A. N. Tiwari, and C. Vignali, "Influence of deposition conditions on the thermal stability of ZnO:Al films grown by rf magnetron sputtering," *Journal of Vacuum Science and Technology A*, vol. 19, no. 1, pp. 171–174, 2001.
- [8] D. A. King, "Thermal desorption from metal surfaces: a review," *Surface Science*, vol. 47, no. 1, pp. 384–402, 1975.
- [9] B. Hokkanen, S. Funk, U. Burghaus, A. Ghicov, and P. Schmuki, "Adsorption kinetics of alkanes on TiO₂ nanotubesarray—structure-activity relationship," *Surface Science*, vol. 601, no. 19, pp. 4620–4628, 2007.
- [10] K. Higuchia, K. Yamamoto, H. Kajioka et al., "Remarkable hydrogen storage properties in three-layered Pd/Mg/Pd thin films," *Journal of Alloys and Compounds*, vol. 330–332, pp. 526–530, 2002.
- [11] N. Patel, A. Kale, P. Mosaner, R. Checchetto, A. Miotello, and G. Das, "Deuterium thermal desorption from Ni-rich deuterated Mg thin films," *Renewable Energy*, vol. 33, no. 2, pp. 232–236, 2008.
- [12] S. C. Chang, T. C. Lin, T. S. Li et al., "Fluorine thermal stability of ZnO:F films investigated by thermal desorption spectroscopy," in *Proceedings of the International Conference on Electronic Materials and Packaging (EMAP '08)*, pp. 25–28, Taipei, Taiwan, October 2008.
- [13] C. Guillén and J. Herrero, "Optical, electrical and structural characteristics of Al:ZnO thin films with various thicknesses deposited by DC sputtering at room temperature and annealed in air or vacuum," *Vacuum*, vol. 84, no. 7, pp. 924–929, 2010.
- [14] S. C. Chang, G. W. Jian, S. H. Huang, T. S. Li, and T. C. Lin, "Some special phenomena observed from in-line sputtered aluminum doped zinc oxide films," in *Proceedings of the 5th International Microsystems, Packaging, Assembly and Circuits Technology Conference (IMPACT '10)*, pp. 1–4, Taipei, Taiwan, October 2010.
- [15] Y. M. Hu, C. W. Lin, and J. C. A. Huang, "Dependences of the Al thickness and annealing temperature on the structural, optical and electrical properties in ZnO/Al multilayers," *Thin Solid Films*, vol. 497, no. 1-2, pp. 130–134, 2006.
- [16] J. F. Chang, H. L. Wang, and M. H. Hon, "Studying of transparent conductive ZnO:Al thin films by RF reactive magnetron sputtering," *Journal of Crystal Growth*, vol. 211, no. 1, pp. 93–97, 2000.
- [17] M. Chen, X. Wang, Y. H. Yu et al., "X-ray photoelectron spectroscopy and auger electron spectroscopy studies of Al-doped ZnO films," *Applied Surface Science*, vol. 158, no. 1, pp. 134–140, 2000.
- [18] E. Burstein, "Anomalous optical absorption limit in InSb," *Physical Review*, vol. 93, no. 3, pp. 632–633, 1954.
- [19] T. S. Moss, "The interpretation of the properties of indium antimonide," *Proceedings of the Physical Society B*, vol. 67, no. 10, pp. 775–782, 1954.
- [20] G. Fang, D. Li, and B. L. Yao, "Fabrication and vacuum annealing of transparent conductive AZO thin films prepared by DC magnetron sputtering," *Vacuum*, vol. 68, no. 4, pp. 363–372, 2002.



Hindawi

Submit your manuscripts at
<http://www.hindawi.com>

